Journal of Materials Chemistry C

PAPER

View Article Online
View Journal | View Issue

Cite this: J. Mater. Chem. C, 2014, 2, 841

Disperse and disordered: a mexylaminotriazine-substituted azobenzene derivative with superior glass and surface relief grating formation†

Robert Kirby,[ab] Ribal Georges Sabat,[a] Jean-Michel Nunzi[b] and Olivier Lebel*[c]

Received 15th October 2013
Accepted 30th November 2013

DOI: 10.1039/c3tc32034k

www.rsc.org/MaterialsC

Materials containing azobenzene chromophores exhibit photomechanical behaviors, including the formation of surface relief gratings (SRG) caused by irradiation with two interfering laser beams. While azo-functionalized polymers were extensively studied, small molecules offer the advantage of being monodisperse species, which translates into easier synthesis and purification, as well as more uniform behavior. A drawback is that they tend to crystallize and do not always form high-quality thin films. Glass-forming compounds incorporating azobenzene were previously synthesized in several synthetic steps and in low yield. Herein, a Disperse Red 1 (DR1) functionalized with a mexylaminotriazine group is synthesized in 94% yield using a simple and straightforward procedure. It shows both the ability to form extremely stable glassy phases, and the ability to form SRG in the solid state with growth rates and grating heights closely similar to DR1-functionalized polymers.

Introduction

Compounds containing azobenzene moieties are well-known for undergoing photoinduced *cis–trans* isomerisation.[1] In the solid state, this isomerisation at the molecular level translates into macroscopic photomechanical behavior where molecules migrate within the material as a result of diffusion of the azo moieties.[2] One particularly attractive consequence of this phenomenon is the formation of surface relief gratings (SRG), which is induced by the exposure to two interfering coherent laser beams.[3–5] Photoinduced SRG have been targeted for several applications, including holographic data storage,[6,7] distributed feedback lasers,[8] optical sensors and coupling devices,[9,10] and light harvesting structures for photovoltaic cells.[11,12]

While initial studies on the solid-state photophysical behavior of azobenzene-based materials were performed using polymers,[13,14] small molecules possess several advantages, being monodisperse species, they are typically easier to purify, characterize and process, and show more reproducibility in their behavior.[15–20] However, the challenge with small molecules is ensuring that they can form amorphous thin films, and not crystallize over time.[15,16] To this end, azobenzene derivatives capable of forming glassy phases have been synthesized by various groups, and it was demonstrated that such materials show photomechanical properties similar to those of their polymer counterparts.[21–26] On the other hand, current azobenzene-based molecular glasses based on triarylamines suffer from certain limitations. Firstly, their synthesis requires multiple steps and typically give modest overall yields, thereby limiting their commercial potential. Second, some structural screening is required to identify compounds with optimal glass-forming ability (that will not crystallize upon heating or standing).

In contrast to "conventional" molecular glasses, mexylaminotriazine-based molecular glasses are more structurally rigid due to higher symmetry, few degrees of rotational freedom, strong conjugation of amino substituents to the triazine ring, and the presence of groups that can engage in hydrogen bonding according to predictable patterns.[27,28] Despite this structural rigidity, these compounds typically show excellent glass-forming ability and high to extreme resistance to crystallization, in part due to their ability to participate in hydrogen bonding in the solid state, and the high interconversion barriers between conformations due to resonance.[29–31] Both of these features increase the energy required to rearrange the molecules into ordered structures, thereby frustrating crystallization. These derivatives can be readily synthesized from cyanuric chloride, 3,5-dimethylaniline, and other various amines, by nucleophilic substitution.[27,28] In addition, the physical properties of the compounds, including their glass

[a]Department of Physics, Royal Military College of Canada, Kingston, ON, K7K 7B4, Canada. E-mail: sabat@rmc.ca; Fax: +1 613-541-6040; Tel: +1 613-541-6000 ext. 6721

[b]Department of Chemistry, Department of Physics, Queen's University, Kingston, ON, K7L 3N6, Canada. E-mail: nunzijm@queensu.ca; Fax: +1 613-533-6669; Tel: +1 613-533-6749

[c]Department of Chemistry and Chemical Engineering, Royal Military College of Canada, Kingston, ON, K7K 7B4, Canada. E-mail: Olivier.lebel@rmc.ca; Fax: +1 613-542-9489; Tel: +1 613-541-6000 ext. 3694

† Electronic supplementary information (ESI) available. See DOI: 10.1039/c3tc32034k

transition temperatures (T_g), can be easily tuned by modifying their molecular structures, and they can also be designed to incorporate reactive groups that can be used to introduce other functionalities.[32]

As it has been demonstrated that mexylaminotriazine units can be attached to other core moieties to induce glass-forming ability in the latter,[33] they are promising candidates for the design of novel azobenzene glasses. In the present study, a novel azobenzene glass was synthesized in a two-stage, one-step process, without the need for extensive purification, and in 94% yield from a mexylaminotriazine precursor and Disperse Red 1, which are both commercially available, and demonstrate both the superior glass-forming properties of mexylaminotriazine glasses and the ability to form surface relief gratings (SRG) with characteristics and growth rates that are comparable to their polymer counterparts.

Experimental section

General

2-Mexylamino-4-methylamino-6-chloro-1,3,5-triazine was purchased from Solaris Chem, Inc. Ethylenediamine, Disperse Red 1 and DR1–PMMA were purchased from Sigma-Aldrich, *N*,*N*′-carbonyldiimidazole (CDI) was purchased from Oakwood Chemicals, and all solvents were purchased from Caledon Labs. All reagents were used without further purification. Reactions were performed under ambient atmosphere unless otherwise specified. Glass transition temperatures were determined with a TA Instruments 2010 Differential Scanning Calorimeter calibrated with indium at a heating rate of 5 °C min^{-1} from 30 to 200 °C. Values were reported after an initial heating and cooling cycle as the average of two heating runs. FTIR spectra were acquired with thin films cast from CH_2Cl_2 on KBr windows using a Perkin-Elmer Spectrum 65 spectrometer. UV-visible absorption spectra were acquired using a Hewlett-Packard 8453 spectrometer. NMR spectra were acquired on either a 400 MHz Bruker AV400 or on a 300 MHz Varian Oxford spectrometer.

Synthesis of 2-methylamino-4-mexylamino-6-(2-aminoethylamino)-1,3,5-triazine (1)

2-Mexylamino-4-methylamino-6-chloro-1,3,5-triazine (50.0 g, 190 mmol) and ethylenediamine (100 mL) were added in a round-bottomed flask equipped with a magnetic stirrer and a water-jacketed condenser, then the mixture was heated at 80 °C for 18 h. After the mixture was allowed to cool down to room temperature, the unreacted ethylenediamine was evaporated under vacuum. The residue was dissolved in 4 M aqueous HCl, and the precipitate was removed by filtration and washed with H_2O. NaOH pellets were added to the filtrate until the pH became basic (>12), then the mixture was stirred for 30 min, at which time the solvent was decanted. The precipitated product was dissolved in CH_2Cl_2, dried over Na_2SO_4, filtered, and the solvent was thoroughly evaporated under reduced pressure to yield 48.9 g of the title compound (170 mmol, 90%): T_g 58 °C; FTIR (CH_2Cl_2/KBr) 3402, 3275, 3195, 3134, 3013, 2945, 2920, 2866, 1587, 1566, 1549, 1520, 1440, 1396, 1358, 1323, 1300, 1266, 1252, 1189, 1159, 1113, 1065, 1037, 996, 972, 952, 934, 882, 842, 810, 735, 689 cm^{-1}; ^{1}H NMR (300 MHz, $CDCl_3$, 298 K) δ 7.22 (s, 2H), 6.84 (br s, 1H), 6.66 (s, 1H), 5.55 (br s, 1H), 5.02 (br s, 1H), 3.47 (br s, 2H), 2.95 (d, ^3J = 5.3 Hz, 3H), 2.90 (t, ^3J = 5.3 Hz, 2H), 2.29 (s, 6H) ppm; ^{13}C NMR (75 MHz, $CDCl_3$) δ 166.6, 166.3, 164.3, 139.2, 138.1, 124.2, 117.9, 43.4, 41.5, 27.4, 21.4 ppm; HRMS (EI) *m*/*z*: $[M]^+$ calcd. for $C_{14}H_{21}N_7$: 287.1858, found: 287.1851.

Synthesis of DR1–glass 2

To a stirred suspension of *N*,*N*′-carbonyldiimidazole (0.773 g, 4.77 mmol) in dry THF (5 mL) in a dry round-bottomed flask equipped with a magnetic stirrer was slowly added a solution of Disperse Red 1 (1.00 g, 3.18 mmol) in dry THF (10 mL) at ambient temperature, then the mixture was stirred for 18 h under nitrogen atmosphere. CH_2Cl_2 and H_2O were added, then the layers were separated, and the organic layer was washed two more times with copious amounts of H_2O. The organic extract was recovered, dried over Na_2SO_4, filtered, and the solvent was evaporated. The crude residue was redissolved in THF (15 mL), then 2-methylamino-4-mexylamino-6-(2-aminoethylamino)-1,3,5-triazine (1.10 g, 3.82 mmol) was added and the mixture was refluxed for 18 h. The solvent was evaporated, then 1 M aqueous HCl was added, then the precipitated product was collected by filtration and washed with 1 M aq. HCl and H_2O until the effluent was colorless. The residue was dissolved in acetone, then CH_2Cl_2 and aq. $NaHCO_3$ were added. The layers were separated, the organic layer was dried over Na_2SO_4, filtered, and the volatiles were thoroughly evaporated under reduced pressure to yield 1.875 g of pure glass **2** (2.99 mmol, 94%). T_g 71 °C; FTIR (CH_2Cl_2/KBr) 3560, 3272, 2973, 2925, 2869, 2853, 2066, 1688, 1647, 1626, 1600, 1584, 1566, 1511, 1440, 1420, 1389, 1376, 1355, 1334, 1309, 1244, 1189, 1153, 1131, 1102, 1041, 1014, 994, 960, 940, 917, 856, 821, 808, 776, 754, 726, 686 cm^{-1}; ^{1}H NMR (400 MHz, DMSO-d_6, 363 K) δ 8.33 (d, ^3J = 9.3 Hz, 2H), 8.27 (br s, 1H), 7.90 (d, ^3J = 9.1 Hz, 2H), 7.83 (d, ^3J = 9.3 Hz, 2H), 7.39 (s, 2H), 6. 90 (d, ^3J = 9.3 Hz, 2H), 6.84 (br s, 1H), 6.56 (s, 1H), 6.37 (br s, 1H), 6.30 (br s, 1H), 4.20 (t, ^3J = 6.0 Hz, 2H), 3.67 (t, ^3J = 6.0 Hz, 2H), 3.40 (q, ^3J = 7.1 Hz, 2H), 3.24 (q, ^3J = 6.0 Hz, 2H), 2.83 (d, ^3J = 4.8 Hz, 3H), 2.23 (s, 6H), 1.18 (t, ^3J = 7.1 Hz, 3H) ppm; ^{13}C NMR (100 MHz, DMSO-d_6) δ 166.1, 163.9, 156.1, 151.5, 146.7, 142.7, 140.5, 136.9, 126.0, 124.8, 122.6, 122.4, 117.1, 111.5, 61.1, 48.7, 45.0, 40.4, 40.4, 27.2, 21.2, 11.9 ppm; UV-vis (CH_2Cl_2): λ_{max} (ε) 485 nm (28 000); HRMS (ESI) *m*/*z*: $[M + H]^+$ calcd. for $C_{31}H_{38}N_{11}O_4$: 628.3129, found: 628.3103.

Thin film deposition

Thin films of DR1–PMMA and DR1–glass **2** were deposited by spin-coating using a Headway Research spin-coater. Solutions with a concentration of 3 wt% in CH_2Cl_2 were prepared and submitted to mechanical shaking for 1 hour, then filtered with a 50 μm filter. Approximately 3 mL of solution were deposited on a BK7 glass slide with dimensions of 3 × 3 cm^2, at a rate of 1000 rpm for 40 seconds. The films were then dried in a Yamato ADP-21 oven at 95 °C for 5 minutes. Film thicknesses were measured with a Sloan Dektak II D profilometer (model 139961). Powder

X-ray Diffraction patterns of the films were acquired with a Scintag X1 diffractometer using Cu K_α (1.54 Å) between 2.5 and 50° (2θ) and with a step of 0.02° and a scanning rate of 2.00° min^{-1}.

Surface relief grating writing

SRG were formed on thin films of DR1–PMMA and DR1–glass **2** by irradiating the samples with two interfering beams from a Coherent Verdi diode-pumped laser (model 0174-525-52, 5 Watts), one directly incident, one reflected upon a 3 × 3 cm^2 Lloyd mirror placed orthogonally to the sample. The circularly polarized incident beam was collimated, and passed through a variable iris with a 1 cm diameter opening. This yielded a grating area of approximately 0.39 cm^2. First-order diffraction intensity measurements were performed as described in the Results section.

Atomic force microscopy

AFM scans were performed using a Pacific Nanotechnology Nano-R O-020-0002 scanning probe microscope, in tapping mode using mounted cantilever probes (Pacific Nanotechnology model P-MAN-SICT-0).

Results and discussion

Synthesis

Disperse Red 1 was selected as the dye because it is commercially available, its photophysical and photomechanical properties have been extensively studied (in particular as DR1–PMMA), and its remote hydroxy group can be functionalized with minimal perturbation of the optical properties of the chromophore. From a synthetic standpoint, the simplest route to design a molecular glass substituted with a Disperse Red 1 moiety involves reacting the hydroxy group of DR1 with a molecular glass already containing a functionalizable group. Several glass-forming mexylaminotriazine derivatives containing reactive groups have been reported in recent work, some of which can be readily made to participate in a covalent bond-forming reaction with an alcohol.[32] However, none of the glasses reported so far gave satisfactory results: either the yields were too low, expensive or highly toxic reagents were necessary, a large excess of either DR1 or the glass were required, or purification involved chromatography requiring large volumes of solvents.

Carbamoylation with an amino-substituted glass was selected as the synthetic method because it can be performed in one step with roughly stoichiometric amounts of reagents and under ambient conditions. As alkylamines are much more reactive than anilines, new aminoethyl-substituted glass **1** was synthesized from 2-mexylamino-4-methylamino-6-chloro-1,3,5-triazine and excess ethylenediamine in 90% yield according to Scheme 1. As compound **1** is soluble in aqueous acidic media, it can be readily purified by dissolving the crude product in aqueous HCl followed by neutralization.

Glass **1** shows a glass transition temperature (T_g) of 58 °C as measured by Differential Scanning Calorimetry (DSC) with no crystallization upon heating at a rate of 5 °C min^{-1}. A representative DSC scan is shown in Fig. 1a. Glass **1** thus shares the glass-forming ability and high resistance to crystallization shown by other derivatives of the mexylaminotriazine family, even with a single arylamino substituent. It has been shown previously that with a strong glass-promoting "headgroup" at the 2-position of the triazine ring such as the methylamino group, alkylamino groups can occupy the 4- and 6-positions without loss of glass-forming ability.[34]

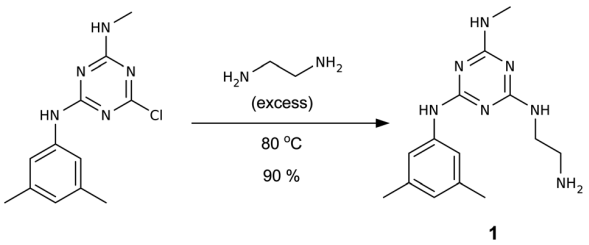

1

Scheme 1 Synthesis of glass precursor **1**.

To bond Disperse Red 1 to glass-forming precursor **1** in a covalent fashion, DR1 was first reacted with

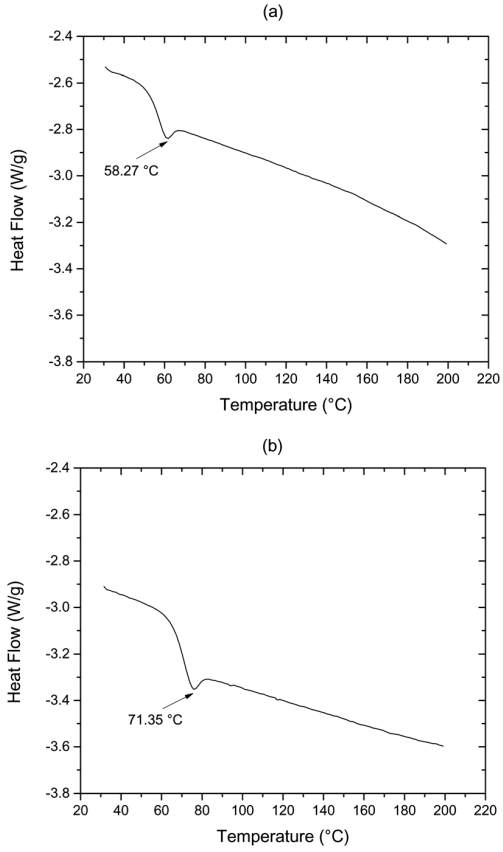

Fig. 1 Representative differential scanning calorimetry scans of (a) compound **1**, and (b) DR1-substituted glass **2**. The scans were recorded at a heating rate of 5 °C min^{-1}. T_g values are indicated. Note the absence of crystallization in both cases.

N,*N*-carbonyldiimidazole (CDI), then the crude intermediate was reacted with glass **1** to afford pure DR1 mexylaminotriazine adduct **2** in 94% yield after an acidic washing which removes unreacted glass **1**, DR1 and imidazole, as shown in Scheme 2.

However, attempts to first react amine **1** with CDI followed by DR1 resulted in the formation of an insoluble precipitate which could not be identified. As expected, azo dye **2** readily forms glasses with a T_g of 71 °C (as measured by DSC with a heating rate of 5 °C min^{-1}) and does not recrystallize upon heating, even with a heating rate as low as 0.5 °C min^{-1}.

A DSC scan of glass-forming dye **2** is shown in Fig. 1b. As expected, the mexylaminotriazine moiety imparted its ability to promote glass formation to the Disperse Red 1 dye, without perturbing the chromophore, as evidenced by the absorption spectra of dye **2** in CH_2Cl_2 solution, shown in Fig. 2a along with the spectra of Disperse Red 1 itself and DR1–PMMA. The absorption of glass **2** in the visible range overlaps almost perfectly that of DR1 (λ_{max} = 485 nm), whereas the absorption maximum of DR1–PMMA is slightly shifted (λ_{max} = 473 nm).

Thin film deposition

Thin films of both DR1–PMMA and DR1–glass **2** were prepared by spin-coating from 3 wt% solutions in CH_2Cl_2 on thick BK7 glass substrates followed by drying in an oven. The solid films yielded thicknesses around 450 nm. The amorphous nature of the film was confirmed with powder X-ray diffraction (PXRD) by the absence of any crystalline peaks as shown in Fig. 3. The PXRD pattern of a sample of compound **2** is also shown and also shows a broad halo, confirming the propensity of the material to adopt a glassy state. It should be noted that DR1–glass **2** dissolved quicker in CH_2Cl_2 and formed more uniform and higher-quality thin films than its polymer counterpart. DR1–PMMA is known to behave differently from one sample to the

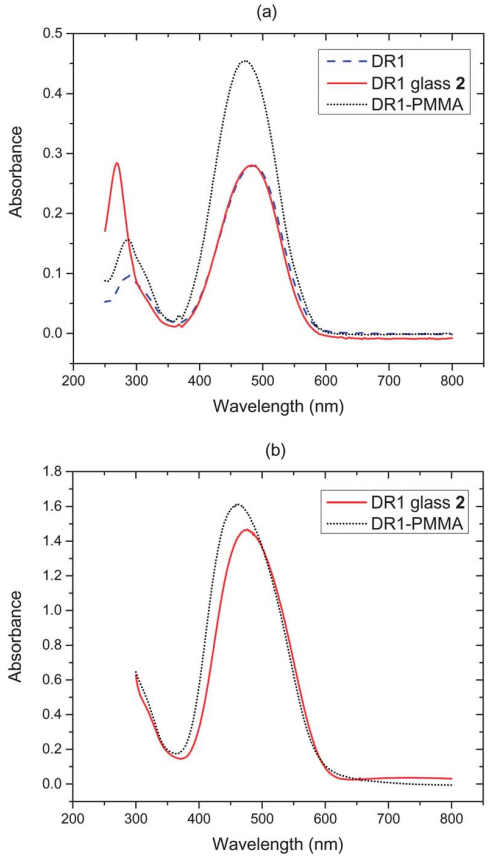

Fig. 2 Absorbance spectra: (a) Disperse Red 1, DR1–glass **2**, and DR1–PMMA in CH_2Cl_2 solution; and (b) thin solid films of DR1–glass **2** and DR1–PMMA. The spectra in CH_2Cl_2 solution were recorded using concentrations of 0.01 mM for DR1 and compound **2**, and 0.0006 wt% for DR1–PMMA.

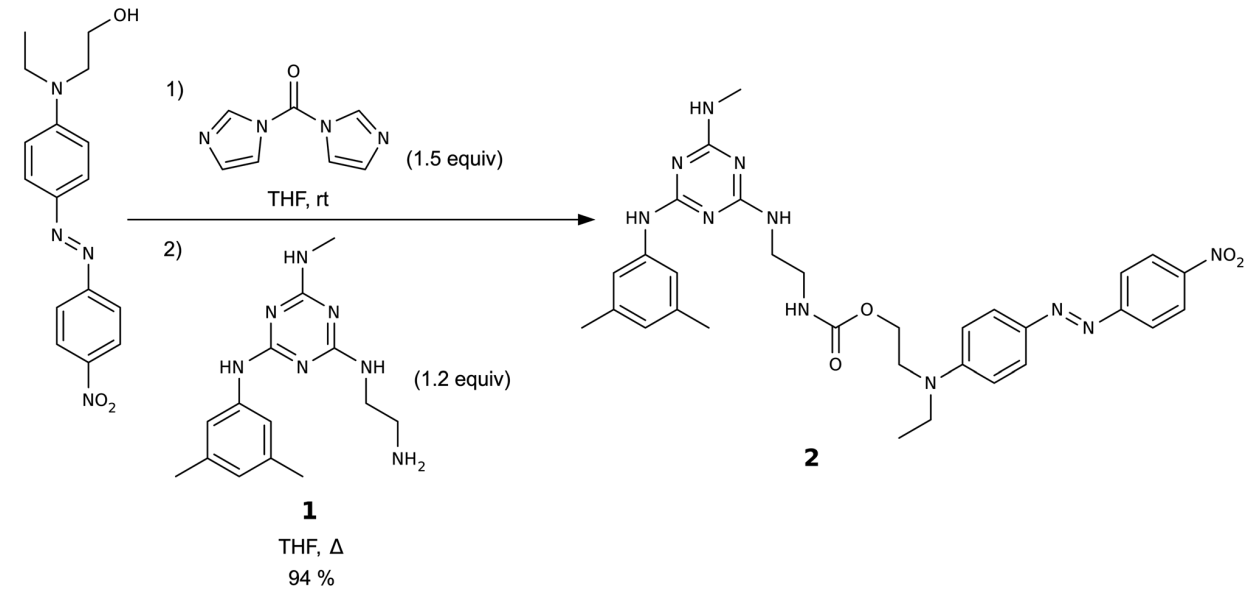

Scheme 2 Synthesis of DR1–glass **2**.

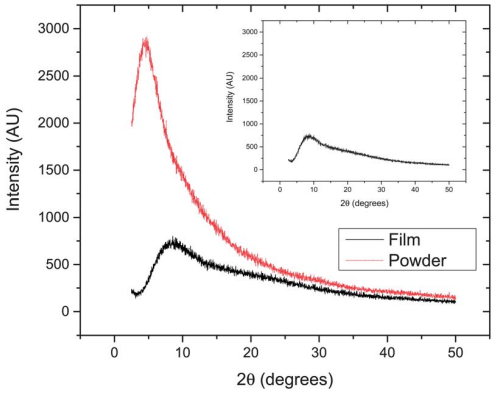

Fig. 3 Powder X-ray Diffraction (PXRD) pattern of a film and a powder sample of DR1–glass **2**. The diffraction pattern of the substrate is shown for comparison.

other depending on chain lengths, which affects thin film formation. This behavior was not observed in films of DR1–glass **2** because of its monodisperse nature. Absorbance spectra of these films are reported in Fig. 2b, from which it can be observed that even in the solid state, the DR1–glass **2** (λ_{max} = 476 nm) mirrors more closely the absorption maximum of DR1 than DR1–PMMA (λ_{max} = 462 nm).

SRG inscription

A circularly polarized 532 nm diode-pumped laser was collimated and incident on a Lloyd mirror where a thin film of either DR1–PMMA or DR1–glass **2** was placed orthogonally to the mirror. The centre of the beam was at the junction of the sample and the mirror, so that half of the beam was immediately incident onto the sample, while the other half was reflected onto the sample, creating an interference pattern on the sample's surface, as previously detailed in the literature.[35] This interference pattern yielded the formation of Surface Relief Gratings (SRG). The grating pitch could be varied by rotating the Lloyd mirror with respect to the writing beam, but for this series of experiments, the pitch was kept constant at 600 nm for all SRG. The depth of the gratings was dependent on the laser exposure time. Fig. 4 shows Atomic Force Microscopy (AFM) scans of SRG on thin films of DR1–PMMA and DR1–glass **2** with laser exposure times of 300 s and 500 s, respectively.

Monitoring of diffraction efficiency *via* probe laser

The time-dependent diffraction efficiency was monitored for both DR1–PMMA and DR1–glass **2** during laser irradiation. To accomplish this, a probe He–Ne laser was incident on the portion of the thin film where the SRG is being inscribed, as illustrated in Fig. 5. As the grating appeared, the first order diffracted beam from the He–Ne laser was mechanically chopped and then incident on a silicon photodetector. The signal of the photodetector was then measured by a lock-in amplifier and recorded by a computer. The diffraction efficiency was obtained by dividing the signal of the first by the zeroth diffraction order.

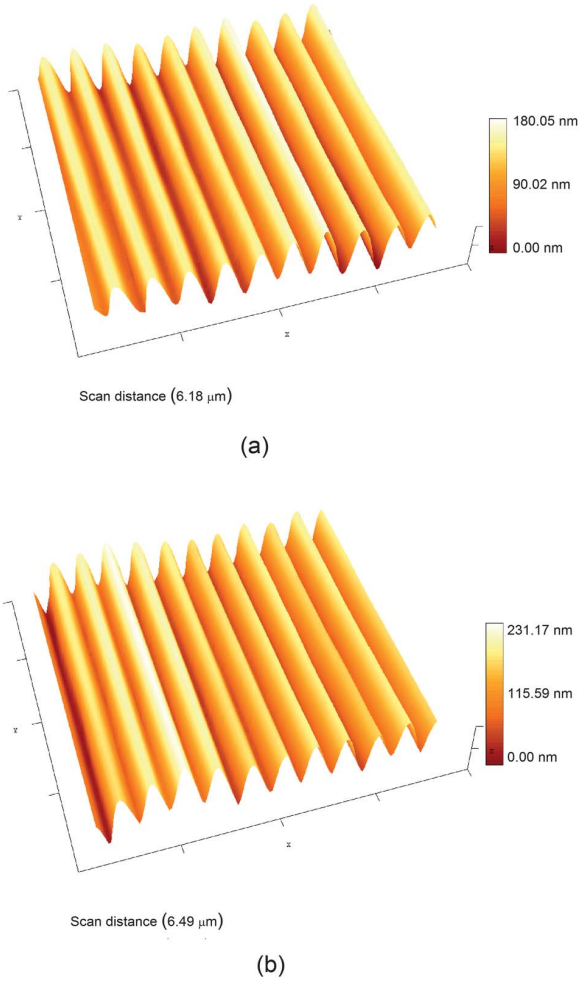

Fig. 4 AFM scans of surface relief gratings written on thin films of (a) DR1–PMMA polymer, and (b) DR1–glass **2**, both with a 600 nm pitch.

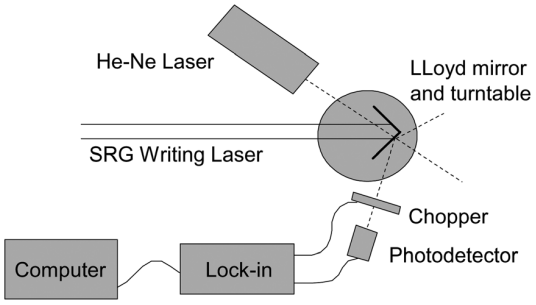

Fig. 5 Experimental set-up for monitoring diffraction efficiency.

The writing laser's irradiance was varied between 50, 83 and 330 mW cm^{-2}, as the diffraction efficiency was monitored. As seen in Fig. 6, a diffraction signal appeared almost immediately after laser illumination in both DR1–glass **2** and DR1–PMMA. This is due to the formation of birefringence volume gratings within the films. Usually, these birefringence gratings appear

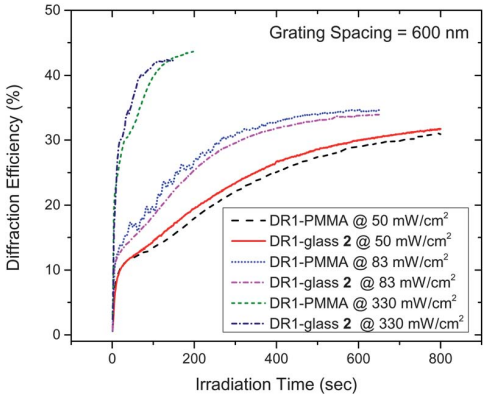

Fig. 6 Diffraction efficiency as a function of irradiation time for DR1–PMMA and DR1–glass **2** at various laser irradiances.

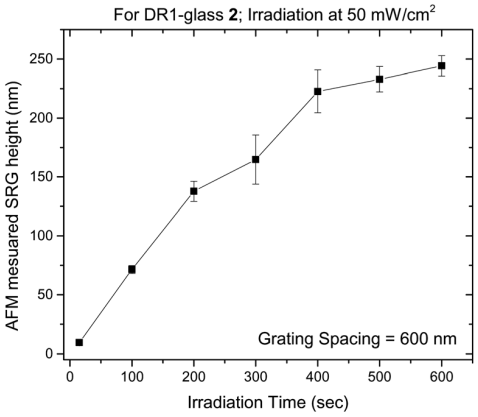

Fig. 7 SRG height as a function of irradiation time for DR1–glass **2**.

quicker than SRG, but are much less stable and produce less overall diffraction. As exposure time increased, the diffraction signal from the birefringence gratings became overshadowed by that of the more stable SRG. Regardless, the respective diffraction efficiencies of DR1–glass **2** and DR1–PMMA were almost identical for all irradiances used. Moreover, the rates of growth observed for both DR1–glass **2** and DR1–PMMA were significantly faster than those observed for other azobenzene-containing glasses previously published in the literature,[21–26] though it is unclear whether this is the result of the experimental setup, or the use in other cases of slightly different chromophores. SRG written on films of both DR1–PMMA and DR1–glass **2** achieve maximum diffraction efficiency at around 44% within 150–200 seconds at an irradiation of 330 mW cm^{-2}. Longer exposure times at this irradiation level yielded grating degradation. Using lower irradiance values of the writing laser only delayed the grating formation until the same diffraction maximum was achieved. Nonetheless, more information can be deduced from the rate of growth at lower irradiance values. For instance, at 50 mW cm^{-2}, after only 10–15 seconds, the diffraction efficiency increased quickly to achieve approximately 10% efficiency, then the rate of growth decreased. This is also evident at 83 mW cm^{-2}, but the initial quick growth plateaus at around 12% efficiency.

Monitoring surface relief grating growth *via* AFM

The SRG height for DR1–glass **2** samples was measured using AFM as a function of laser irradiation time at 50 mW cm^{-2}, as shown in Fig. 7. To reduce uncertainty, each data point in Fig. 7 corresponds to the average of three AFM scans on different locations for each SRG. These results confirm the SRG growth rates shown in Fig. 6 since a similar correlation is observed between the diffraction efficiency and SRG height as a function of laser irradiation time, only after the initial burst in the diffraction signal caused by the birefringence volume gratings.

Temperature effects on the diffraction efficiency

Next, the temperature stability of the SRG on both DR1–PMMA and DR1–glass **2** was investigated. Samples with surface relief gratings were placed on a temperature-regulated hot-plate and heated from room temperature up to around 115 °C with a heating rate of around 10 °C min^{-1}. The diffraction intensity of the first diffracted order was measured in reflection using a chopper, photodetector and a lock-in amplifier. As seen in Fig. 8, a sharp decrease in the diffraction signal occurs at 102 °C and 105 °C for DR1–glass **2** and DR1–PMMA respectively. The sinusoidal undulations in the diffraction signal are due to the thermal expansion of the BK7 glass substrate as it is being heated. The temperatures at which the SRG are erased for both DR1–PMMA and DR1–glass **2** are very similar, and cannot be directly rationalized by the respective T_g of both materials (the T_g of the DR1–PMMA sample used was measured to be 91 °C), which differs by 20 °C. Two likely explanations for this observation are that either (1) the DR1 moieties start undergoing rapid uncontrolled thermal *cis–trans* isomerisation, or (2) DR1–glass **2**, being capable of forming hydrogen bonds in the solid state, even above T_g, shows hindered molecular mobility relative to DR1–PMMA, which leads to slower kinetics of SRG degradation. Further studies are currently underway to determine the origin of these observations, which will allow gaining further insight into the mechanisms of SRG writing and erasure.

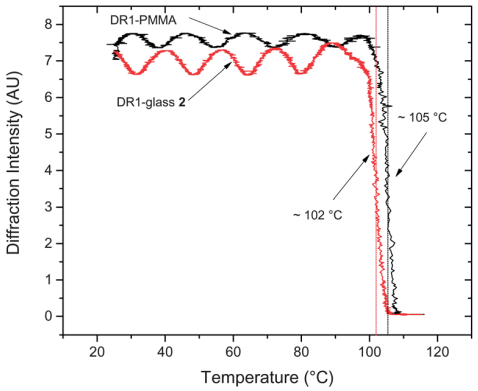

Fig. 8 Diffraction intensity as a function of temperature for DR1–PMMA and DR1–glass **2**.

Conclusions

A novel material incorporating the Disperse Red 1 chromophore and capable of forming stable glassy phases, DR1–glass, was synthesized using a glass-forming precursor. The synthetic procedure used is extremely appealing because it is facile, robust, cost-effective, high-yielding, and the product can be easily purified. The optical properties of the DR1 chromophore are not perturbed by the glass moiety, and the material can easily be processed from solution into high-quality thin films. SRGs can be readily inscribed onto the surface of thin films of DR1–glass, and its photophysical behavior was found to closely mirror that of polymer-supported DR1. As polymers functionalized with DR1 units are used extensively for both their photomechanical and non-linear optic properties, DR1–glass constitutes an extremely exciting new material that shares the photophysical properties of DR1, the thin film- and glass-forming properties of polymers, and the monodisperse, well-defined nature of small molecules. Moreover, the synthetic strategy used herein proved highly efficient, and shows promise for the design and synthesis of molecular glasses incorporating other functional materials. Future work will consist in developing azo-glasses featuring extended spectral sensitivities: red-shifted absorptions that would increase the spectral range of the SRG formation process, as well as blue shifted absorptions that would increase both the transparency range of the SRGs and their stability under ordinary light. Another possibility offered by the ease of functionalization of these glass-forming compounds is to develop multifunctional materials combining opto-electronic functions with the SRGs.

Acknowledgements

The authors would like to thank the Academic Research Programme (ARP) of RMC and the Discovery Grants Program from the Natural Sciences and Engineering Research Council (NSERC #327116) for funding. The authors would also like to thank Dr René Gagnon (Université de Sherbrooke) and Dr Yimin She (Queen's University) for mass spectrometry analyses, Robert Whitehead (RMC) for PXRD acquisition, as well as Dr Paul Rochon (Royal Military College of Canada) for useful discussions.

Notes and references

1 *Photoreactive Organic Thin Films*, ed. Z. Sekkat and W. Knoll, Academic Press, Amsterdam, 2002.
2 *Smart Light-Responsive Materials: Azobenzene-Containing Polymers and Liquid Crystals*, ed. Y. Zhao and T. Ikeda, Wiley, Hoboken, 2009.
3 C. Cojocariu and P. Rochon, *Pure Appl. Chem.*, 2004, **76**, 1479–1497.
4 N. K. Viswanathan, D. Y. Kim, S. Bian, J. Williams, W. Liu, L. Li, L. Samuelson, J. Kumar and S. K. Tripathy, *J. Mater. Chem.*, 1999, **9**, 1941–1955.
5 A. Priimagi and A. Shevchenko, *J. Polym. Sci., Part B: Polym. Phys.*, 2013, DOI: 10.1002/polb.23390.
6 F. Gallego-Gomez, F. Del Monte and K. Meerholz, *Nat. Mater.*, 2008, **7**, 490–497.
7 S. Ahmadi-Kanjani, R. Barille, S. Dabos-Seignon, J. M. Nunzi, E. Ortyl and S. Kucharski, *Opt. Lett.*, 2005, **30**, 1986–1988.
8 L. Rocha, V. Dumarcher, C. Denis, P. Raimond, C. Fiorini and J. M. Nunzi, *J. Appl. Phys.*, 2001, **89**, 3067–3069.
9 J. P. Monteiro, J. Ferreira, R. G. Sabat, P. Rochon, M. J. L. Santos, J. Marcos and E. M. Girotto, *Sens. Actuators, B*, 2012, **174**, 270–273.
10 C. Hubert, C. Fiorini-Debuisschert, I. Hassiaoui, L. Rocha, P. Raimond and J. M. Nunzi, *Appl. Phys. Lett.*, 2005, **87**, 191105.
11 J. Jefferies and R. G. Sabat, *Prog. Photovolt: Res. Appl.*, 2012, DOI: 10.1002/pip.2326.
12 C. Cocoyer, L. Rocha, L. Sicot, B. Geffroy, R. de Bettignies, C. Sentein, C. Fiorini-Debuisschert and P. Raimond, *Appl. Phys. Lett.*, 2006, **88**, 133108.
13 A. Natansohn and P. Rochon, *Adv. Mater.*, 1999, **11**, 1387–1391.
14 A. Natansohn and P. Rochon, *Chem. Rev.*, 2002, **102**, 4139–4175.
15 C. A. Angell, *Science*, 1995, **267**, 1924–1935.
16 M. D. Ediger, C. A. Angell and S. R. Nagel, *J. Phys. Chem.*, 1996, **100**, 13200–13212.
17 Y. Shirota, *J. Mater. Chem.*, 2000, **10**, 1–25.
18 P. Strohriegl and J. V. Grazulevicius, *Adv. Mater.*, 2002, **14**, 1439–1452.
19 Y. Shirota and H. Kageyama, *Chem. Rev.*, 2007, **107**, 953–1010.
20 R. Lygaitis, V. Getautis and J. V. Grazulevicius, *Chem. Soc. Rev.*, 2008, **37**, 770–788.
21 H. Nakano, T. Takahashi, T. Kadota and Y. Shirota, *Adv. Mater.*, 2002, **14**, 1157–1160.
22 E. Ishow, B. Lebon, Y. He, X. Wang, L. Bouteiller, L. Galmiche and K. Nakatani, *Chem. Mater.*, 2006, **18**, 1261–1267.
23 H. Nakano, T. Tanino, T. Takahashi, H. Ando and Y. Shirota, *J. Mater. Chem.*, 2008, **18**, 242–246.
24 E. Ishow, R. Camacho-Aguilera, J. Guerin, A. Brosseau and K. Nakatani, *Adv. Funct. Mater.*, 2009, **19**, 796–804.
25 H. Nakano, T. Takahashi, T. Tanino and Y. Shirota, *Dyes Pigm.*, 2010, **84**, 102–107.
26 A. Jacquart, E. Morin, F. Yang, B. Geffroy and E. Ishow, *Dyes Pigm.*, 2012, **92**, 790–797.
27 O. Lebel, T. Maris, M.-È. Perron, E. Demers and J. D. Wuest, *J. Am. Chem. Soc.*, 2006, **128**, 10372–10373.
28 J. D. Wuest and O. Lebel, *Tetrahedron*, 2009, **65**, 7393–7402.
29 R. Wang, C. Pellerin and O. Lebel, *J. Mater. Chem.*, 2009, **19**, 2747–2753.
30 A. Plante, D. Mauran, S. P. Carvalho, J. Y. S. D. Pagé, C. Pellerin and O. Lebel, *J. Phys. Chem. B*, 2009, **113**, 14884–14891.
31 A. Plante, S. Palato, O. Lebel and A. Soldera, *J. Mater. Chem. C*, 2013, **1**, 1037–1042.
32 R. N. Eren, A. Plante, A. Meunier, A. Laventure, Y. Huang, J. G. Briard, K. J. Creber, C. Pellerin, A. Soldera and O. Lebel, *Tetrahedron*, 2012, **68**, 10130–10144.
33 A. Meunier and O. Lebel, *Org. Lett.*, 2010, **12**, 1896–1899.
34 A. Laventure, A. Soldera, C. Pellerin and O. Lebel, *New J. Chem.*, 2013, **37**, 3881–3889.
35 P. Rochon, E. Batalla and A. Natansohn, *Appl. Phys. Lett.*, 1995, **66**, 136–138.